

NASA/TM-2005-213547



# An Engineering Solution for using Coarse Meshes in the Simulation of Delamination With Cohesive Zone Models

*Albert Turon*  
*University of Girona, Girona, Spain*

*Carlos G. Dávila*  
*Langley Research Center, Hampton, Virginia*

*Pedro P. Camanho*  
*University of Porto, Porto, Portugal*

*Josep Costa*  
*University of Girona, Girona, Spain*

## The NASA STI Program Office . . . in Profile

Since its founding, NASA has been dedicated to the advancement of aeronautics and space science. The NASA Scientific and Technical Information (STI) Program Office plays a key part in helping NASA maintain this important role.

The NASA STI Program Office is operated by Langley Research Center, the lead center for NASA's scientific and technical information. The NASA STI Program Office provides access to the NASA STI Database, the largest collection of aeronautical and space science STI in the world. The Program Office is also NASA's institutional mechanism for disseminating the results of its research and development activities. These results are published by NASA in the NASA STI Report Series, which includes the following report types:

- **TECHNICAL PUBLICATION.** Reports of completed research or a major significant phase of research that present the results of NASA programs and include extensive data or theoretical analysis. Includes compilations of significant scientific and technical data and information deemed to be of continuing reference value. NASA counterpart of peer-reviewed formal professional papers, but having less stringent limitations on manuscript length and extent of graphic presentations.
- **TECHNICAL MEMORANDUM.** Scientific and technical findings that are preliminary or of specialized interest, e.g., quick release reports, working papers, and bibliographies that contain minimal annotation. Does not contain extensive analysis.
- **CONTRACTOR REPORT.** Scientific and technical findings by NASA-sponsored contractors and grantees.

- **CONFERENCE PUBLICATION.** Collected papers from scientific and technical conferences, symposia, seminars, or other meetings sponsored or co-sponsored by NASA.
- **SPECIAL PUBLICATION.** Scientific, technical, or historical information from NASA programs, projects, and missions, often concerned with subjects having substantial public interest.
- **TECHNICAL TRANSLATION.** English-language translations of foreign scientific and technical material pertinent to NASA's mission.

Specialized services that complement the STI Program Office's diverse offerings include creating custom thesauri, building customized databases, organizing and publishing research results ... even providing videos.

For more information about the NASA STI Program Office, see the following:

- Access the NASA STI Program Home Page at <http://www.sti.nasa.gov>
- E-mail your question via the Internet to [help@sti.nasa.gov](mailto:help@sti.nasa.gov)
- Fax your question to the NASA STI Help Desk at (301) 621-0134
- Phone the NASA STI Help Desk at (301) 621-0390
- Write to:  
NASA STI Help Desk  
NASA Center for AeroSpace Information  
7121 Standard Drive  
Hanover, MD 21076-1320

NASA/TM-2005-213547



# An Engineering Solution for using Coarse Meshes in the Simulation of Delamination With Cohesive Zone Model

*Albert Turon*  
*University of Girona, Girona, Spain*

*Carlos G. Dávila*  
*Langley Research Center, Hampton, Virginia*

*Pedro P. Camanho*  
*University of Porto, Porto, Portugal*

*Josep Costa*  
*University of Girona, Girona, Spain*

National Aeronautics and  
Space Administration

Langley Research Center  
Hampton, Virginia 23681-2199

March 2005

Available from:

NASA Center for AeroSpace Information (CASI)  
7121 Standard Drive  
Hanover, MD 21076-1320  
(301) 621-0390

National Technical Information Service (NTIS)  
5285 Port Royal Road  
Springfield, VA 22161-2171  
(703) 605-6000

# An Engineering Solution for using Coarse Meshes in the Simulation of Delamination with Cohesive Zone Models

A. Turon <sup>a</sup>, C.G. Dávila <sup>b</sup>, P.P. Camanho <sup>c</sup>, J. Costa <sup>a</sup>

<sup>a</sup>*AMADE, Polytechnic School, University of Girona, Campus Montilivi s/n, 17071 Girona, Spain*

<sup>b</sup>*NASA Langley Research Center, Hampton, Virginia, U.S.A.*

<sup>c</sup>*DEMEGI, Faculdade de Engenharia, Universidade do Porto, Rua Dr. Roberto Frias, 4200-465, Porto, Portugal*

---

## Abstract

This paper presents a methodology to determine the parameters used in the simulation of delamination in composite materials using decohesion finite elements. A closed-form expression is developed to define the stiffness of the cohesive layer. A novel procedure that allows the use of coarser meshes of decohesion elements in large-scale computations is proposed. The procedure ensures that the energy dissipated by the fracture process is correctly computed. It is shown that coarse-meshed models defined using the approach proposed here yield the same results as the models with finer meshes normally used in the simulation of fracture processes.

---

## 1 Introduction

Delamination, or interfacial cracking between composite layers, is one of the most common types of damage in laminated fibre-reinforced composites due to their relatively weak interlaminar strengths. Delamination may arise under various circumstances, such as low velocity impacts, or bearing loads in structural joints. The delamination failure mode is particularly important for the structural integrity of composite structures because it is difficult to detect during inspection.

The simulation of delamination using the finite element method (FEM) is normally performed using the Virtual Crack Closure Technique (VCCT) [1], or decohesion finite elements [2]-[3].

The VCCT is based on the assumption that the energy released during delamination propagation equals the work required to close the crack back to its original position. Based on this assumption, the single-mode components of the energy release rate are computed from the nodal forces and nodal relative displacements [1]. Delamination growth is predicted when a combination of the components of the energy release rate is equal to a critical value.

There are some difficulties when using the VCCT in the simulation of progressive delamination. The calculation of fracture parameters requires nodal variable and topological information from the nodes ahead and behind the crack front. Such calculations are tedious to perform and may require remeshing for crack propagation.

The use of decohesion finite elements can overcome some of the above difficulties. Decohesion finite elements can predict both the onset and non-self-similar propagation of delamination. However, the simulation of progressive delamination using decohesion elements poses numerical difficulties related with the proper definition of the stiffness of the cohesive layer, the requirement of extremely refined meshes, and the convergence difficulties associated with problems involving softening constitutive models.

This work addresses the proper definition of interface stiffness and proposes a novel procedure to allow the use of coarse meshes in the simulation of delamination.

A brief description of the kinematics and constitutive model of a previously proposed decohesion element [2]-[3] is presented. A closed-form expression is developed, replacing the empirical definitions of the stiffness of the cohesive layer that are normally used. A solution to use coarse meshes in the simulation of delamination is proposed. It is demonstrated that the proposed solution can yield results as accurate as the ones obtained using very refined meshes.

## **2 Cohesive zone model approach**

The Cohesive Zone Model (CZM) approach [4]-[6] is one of the most commonly used tools to investigate interfacial fracture. The CZM approach assumes that a cohesive damage zone, or softening plasticity, develops near the crack tip.

The CZM links the microstructural failure mechanism to the continuum fields governing bulk deformations. Thus, a CZM is characterized by the properties of the bulk material, the crack initiation condition, and the crack evolution function.

Cohesive damage zone models relate traction to displacement jumps at an interface where a crack may occur. Damage initiation is related to the interfacial strength, i.e., the maximum traction on the traction-displacement jump relation. When the area under the traction-displacement jump relation is equal to the fracture toughness, the traction is reduced to zero, and new crack surfaces are formed.

### 2.1 Kinematics and constitutive relation of cohesive zone models

The cohesive zone model used here was previously proposed by the authors [2]-[3]. A brief description of the model, with special focus on the kinematics and constitutive damage model, is presented.

Consider a domain  $\Omega$  containing a material discontinuity,  $\Gamma_d$ , which divides the domain  $\Omega$  into two parts,  $\Omega_+$  and  $\Omega_-$ , as shown in Figure 1.

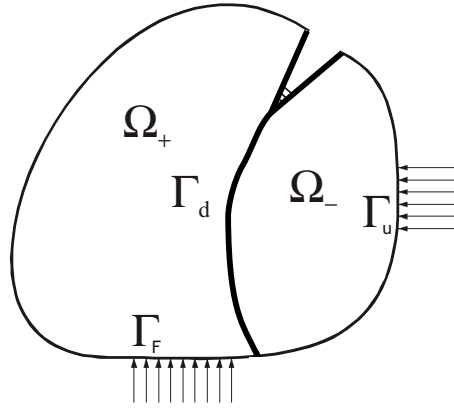


Fig. 1. Body  $\Omega$  crossed by a material discontinuity  $\Gamma_d$  in the undeformed configuration.

Prescribed tractions,  $t_i$ , are imposed on the boundary  $\Gamma_F$ , whereas prescribed displacements are imposed on the boundary  $\Gamma_u$ . The stress field inside the domain,  $\sigma_{ij}$ , is related to the external loading and the closing tractions  $\tau_j^+$ ,  $\tau_j^-$  in the material discontinuity through the equilibrium equations:

$$\sigma_{ij,j} = 0 \text{ in } \Omega \quad (1)$$

$$\sigma_{ij}n_j = t_i \text{ on } \Gamma_F \quad (2)$$

$$\sigma_{ij}n_j^+ = \tau_i^+ = -\tau_i^- = \sigma_{ij}n_j^- \text{ on } \Gamma_d \quad (3)$$

The displacement jump across the interface of the material discontinuity required in the constitutive model,  $\llbracket u_i \rrbracket$ , can be obtained as a function of the

displacement of the points located on the top and bottom side of the interface,  $u_i^+$  and  $u_i^-$  respectively:

$$\llbracket u_i \rrbracket = u_i^+ - u_i^- \quad (4)$$

where  $u_i^\pm$  are the displacements with respect to the fixed Cartesian coordinate system. A co-rotational formulation is used in order to express the components of the displacement jumps with respect to the deformed interface. The coordinates  $\bar{x}_i$  of the deformed interface can be written as [7]:

$$\bar{x}_i = X_i + \frac{1}{2} (u_i^+ + u_i^-) \quad (5)$$

where  $X_i$  are the coordinates of the undeformed interface.

The components of the displacement jump tensor in the local coordinate system on the deformed interface,  $\Delta_m$ , are expressed in terms of the displacement field in global coordinates:

$$\Delta_m = \Theta_{mi} \llbracket u_i \rrbracket \quad (6)$$

where  $\Theta_{mi}$  is the rotation tensor.

The constitutive operator of the interface,  $D_{ji}$ , relates the element tractions,  $\tau_j$ , to the displacement jumps,  $\Delta_i$ :

$$\tau_j = D_{ji} \Delta_i \quad (7)$$

A requirement of the constitutive relations of cohesive zone models is that the energy dissipated in the process of fracture needs to be computed accurately.

Under single-mode loading, controlled energy dissipation is achieved assuring that the area under the traction-displacement jump relation equals the corresponding fracture toughness, as illustrated in Figure 2.

Under mixed-mode loading, a criterion established in terms of an interaction between components of the energy release rate needs to be used.

There are several types of constitutive operators presented in the literature, depending on the constitutive equations used for the simulation of the delamination: Tvergaard and Hutchinson [8] used a trapezoidal law, Cui and Wisnom [9] proposed a perfectly plastic rule, Needleman used a polynomial

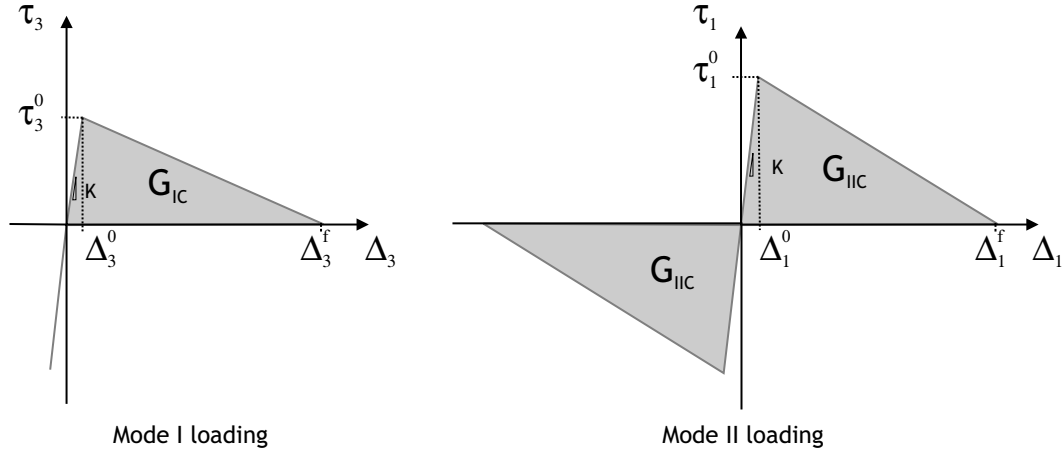


Fig. 2. *Constitutive equations under Mode I and Mode II loading.*

law, [10], and later an exponential law [11]. In this paper, a bilinear constitutive equation is used.

The constitutive damage model used here, formulated in the context of Damage Mechanics (DM), was previously proposed by the authors [2],[3]. All the details of the constitutive model are presented in reference [2] and [3] and will not be repeated here.

The constitutive model prevents interpenetration of the faces of the crack during closing, and a Fracture Mechanics-based criterion is used to predict crack propagation. The formulation of the damage model is summarized in Table 1, where  $\psi$  and  $\psi^0$  are the free energy per unit surface of the damaged and undamaged interface, respectively.  $\bar{\delta}_{ij}$  is the Kronecker delta, and  $d$  is a scalar damage variable. The parameter  $\lambda$  is the norm of the displacement jump tensor (also called *equivalent displacement jump norm*), and it is used to compare different stages of the displacement jump state so that it is possible to define such concepts as ‘loading’, ‘unloading’ and ‘reloading’. The equivalent displacement jump is a non-negative and continuous function, defined as:

$$\lambda = \sqrt{\langle \Delta_3 \rangle^2 + (\Delta_{shear})^2} \quad (8)$$

where  $\langle \cdot \rangle$  is the MacAuley bracket defined as  $\langle x \rangle = \frac{1}{2}(x + |x|)$ .  $\Delta_3$  is the displacement jump in mode I, i.e., normal to midplane, and  $\Delta_{shear}$  is the Euclidean norm of the displacement jump in mode II and in mode III:

$$\Delta_{shear} = \sqrt{(\Delta_1)^2 + (\Delta_2)^2} \quad (9)$$

Table 1. Definition of the constitutive model.

Free Energy	$\psi(\Delta, \mathbf{d}) = (1 - \mathbf{d}) \psi^0(\Delta_i) - \mathbf{d} \psi^0(\bar{\delta}_{3i} \langle -\Delta_3 \rangle)$
Constitutive equation	$\tau_i = \frac{\partial \psi}{\partial \Delta_i} = (1 - \mathbf{d}) \bar{\delta}_{ij} K \Delta_j - \mathbf{d} \bar{\delta}_{ij} K \bar{\delta}_{3j} \langle -\Delta_3 \rangle$
Displacement jump norm	$\lambda = \sqrt{\langle \Delta_3 \rangle^2 + (\Delta_{shear})^2}$
Damage criterion	$\bar{F}(\lambda^t, r^t) := \mathbf{G}(\lambda^t) - \mathbf{G}(r^t) \leq 0 \quad \forall t \geq 0$
	$\mathbf{G}(\lambda) = \frac{\Delta^f(\lambda - \Delta^0)}{\lambda(\Delta^f - \Delta^0)}$
Evolution law	$\dot{\mathbf{d}} = \dot{\mu} \frac{\partial \bar{F}(\lambda, r)}{\partial \lambda} = \dot{\mu} \frac{\partial \mathbf{G}(\lambda)}{\partial \lambda} \quad ; \quad \dot{r} = \dot{\mu}$
Load/unload conditions	$\dot{\mu} \geq 0 \quad ; \quad \bar{F}(\lambda^t, r^t) \leq 0 \quad ; \quad \dot{\mu} \bar{F}(\lambda^t, r^t) = 0$
	$r^t = \max\{r^0, \max_s \lambda^s\} \quad 0 \leq s \leq t$

The evolution of damage is defined by  $\mathbf{G}(\cdot)$ , a suitable monotonic scalar function, ranging from 0 to 1.  $\dot{\mu}$  is a damage consistency parameter used to define loading-unloading conditions according to the Kuhn-Tucker relations.  $r^t$  is the damage threshold for the current time,  $t$ , and  $r^0$  denotes the initial damage threshold.

$\Delta^0$  is the onset displacement jump, and it is equal to the initial damage threshold  $r^0$ . The initial damage threshold is obtained from the formulation of the initial damage surface or initial damage criterion.  $\Delta^f$  is the final displacement jump, and it is obtained from the formulation of the propagation surface or propagation criterion [2]-[3].

The formulation proposed allows an explicit integration of the constitutive model. The algorithm is implemented as shown in Table 2.

Table 2. Algorithm of the constitutive model.

---



---

**Initial data for time  $t+1$**

Material properties:  $G_{IC}, G_{IIC}, G_{IIIc}, E, \eta, \tau_{shear}^0, \tau_3^0$

Current values:  $\Delta_3, \Delta_{shear}, d^t$

**1. Mixed-mode ratios:**  $\beta = \frac{\Delta_{shear}}{\langle \Delta_3 \rangle + \Delta_{shear}} \quad ; \quad B = \frac{\beta^2}{1+2\beta^2-2\beta}$

**2. Pure mode onset displacement jump:**  $\Delta_i^0 = \frac{\tau_i^0}{K} \quad i = 3, shear$

**3. Mixed-mode onset displacement jump:**  $\Delta^0 = \sqrt{(\Delta_3^0)^2 + [(\Delta_{shear}^0)^2 - (\Delta_3^0)^2] [B]^\eta}$

**4. Mixed-mode final displacement jump:**  $\Delta^f = \frac{2}{K\Delta^0} [G_{Ic} + (G_{IIC} - G_{Ic}) [B]^\eta]$

**5. Displacement jump norm:**  $\lambda = \sqrt{\langle \Delta_3 \rangle^2 + (\Delta_{shear})^2}$

**6. Update internal variables:**  $r^t = \frac{\Delta^0 \Delta^f}{\Delta^f - d^t [\Delta^f - \Delta^0]} \quad ; \quad r^{t+1} = \max \{ r^t, \lambda \}$

$$d^{t+1} = \frac{\Delta^f (r^{t+1} - \Delta^0)}{r^{t+1} (\Delta^f - \Delta^0)}$$

**7. Compute tractions:**  $\tau_i = D_{ij} \Delta_j = \bar{\delta}_{ij} K \left[ 1 - d \left( 1 + \bar{\delta}_{3j} \frac{\langle -\Delta_j \rangle}{\Delta_j} \right) \right] \Delta_j$

**8. Compute tangent stiffness tensor:**

$$D_{ij}^{\tan} = \begin{cases} \left\{ D_{ij} - K \left[ 1 + \bar{\delta}_{3j} \frac{\langle -\Delta_j \rangle}{\Delta_j} \right] \left[ 1 + \bar{\delta}_{3i} \frac{\langle -\Delta_i \rangle}{\Delta_i} \right] \frac{\Delta^f \Delta^0}{\Delta^f - \Delta^0} \frac{1}{\lambda^3} \Delta_i \Delta_j \right\} & , r^t < \lambda < \Delta^f \\ D_{ij} & , r^t > \lambda \text{ or } \Delta^f < \lambda \end{cases}$$


---



---

Further detail regarding the damage model used here can be found in references [2]-[3].

## 2.2 Cohesive zone model and FEM

In a finite element model using the CZM approach, the complete material description is separated into fracture properties captured by the constitutive model of the cohesive surface and the properties of the bulk material, captured by the continuum regions.

There are two conditions to obtain a successful FEM simulation using CZM [12]: (a) The cohesive contribution to the global compliance should be small enough to avoid the introduction of a fictitious compliance to the model, and (b) the element size needs to be less than the cohesive zone length.

### (a) Stiffness of the cohesive zone model

Different guidelines have been proposed for selecting the stiffness of the interface. Daudeville et al. [13] calculated the stiffness in terms of the thickness and the elastic modulus of the interface. The interface thickness between plies is a very small resin-rich region; therefore, the interface stiffness obtained from the Daudeville equations is very high. Zou et al. [14], based on their own experience, proposed a value for the interface stiffness between  $10^4$  and  $10^7$  times the value of the interfacial strength per unit length. Camanho and Dávila [15] obtained accurate predictions using a value of  $10^6 \text{N/mm}^3$ .

The effective elastic properties of the composite depend on the properties of both the cohesive surfaces and the bulk constitutive relations. Although the compliance of the cohesive surfaces can contribute to the global deformation, its only purpose is to simulate fracture. Moreover, the elastic properties of the cohesive surfaces are mesh-dependent because the surface relations exhibit an inherent length scale that is absent in homogeneous deformations [16].

If the cohesive contribution to the compliance is not small enough compared to that of the volumetric constitutive relation, a stiff connection between two neighboring layers before delamination initiation is not assured. The effect of compliance of the interface on the bulk properties of a laminate is illustrated in the one-dimensional model shown in Figure 3. The traction continuity condition requires:

$$\sigma = E_3 \varepsilon = K \Delta \quad (10)$$

where  $\sigma$  is the traction on the surface,  $t$  is the thickness of an adjacent sub-laminate,  $\varepsilon = \frac{\delta t}{t}$  is the transverse strain,  $K$  is the interface stiffness that relates the resulting tractions at the interface with the opening displacement  $\Delta$ , and  $E_3$  is the through-the-thickness Young's modulus of the material. For a transversely isotropic material  $E_3 = E_2$ .

The effective strain of the composite is:

$$\varepsilon_{\text{eff}} = \frac{\delta t}{t} + \frac{\Delta}{t} = \varepsilon + \frac{\Delta}{t} \quad (11)$$

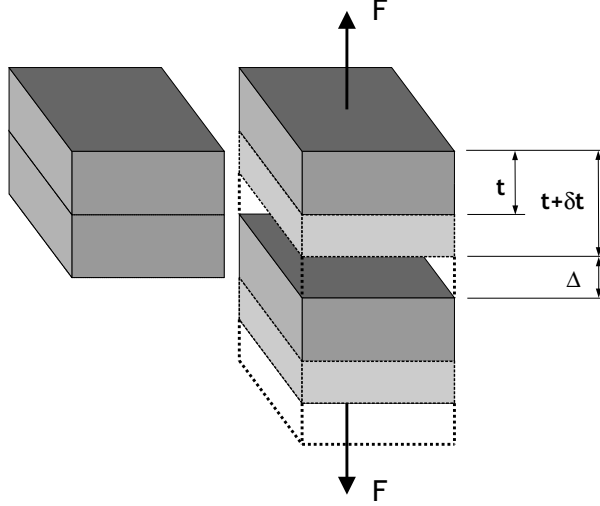


Fig. 3. Influence of the cohesive surface on the deformation.

Since the traction continuity condition requires that  $\sigma = E_{\text{eff}}\varepsilon_{\text{eff}}$ , the equivalent Young's modulus  $E_{\text{eff}}$  can be written as a function of the Young's modulus of the material, the mesh size, and the interface stiffness. Using equations (10) and (11), the effective Young's modulus can be written as:

$$E_{\text{eff}} = E_3 \left( \frac{1}{1 + \frac{E_3}{Kt}} \right) \quad (12)$$

The effective elastic properties of the composite will not be affected by the cohesive surface whenever the inequality  $E_3 \ll Kt$  is being accomplished, i.e:

$$K = \frac{\alpha E_3}{t} \quad (13)$$

where  $\alpha$  is a parameter much larger than 1 ( $\alpha \gg 1$ ). However, large values of the interface stiffness may cause numerical problems, such as spurious oscillations of the tractions [17]. Thus, the interface stiffness should be large enough to provide a reasonable stiffness but small enough to avoid numerical problems such as spurious oscillations of the tractions in an element.

The ratio between the value of the Young modulus obtained with equation (12) and the Young modulus of the material, as a function of the parameter

$\alpha$  is shown in Figure 4. For values of  $\alpha$  greater than 50, the loss of stiffness due to the presence of the interface is less than 2% (see Fig. 4).

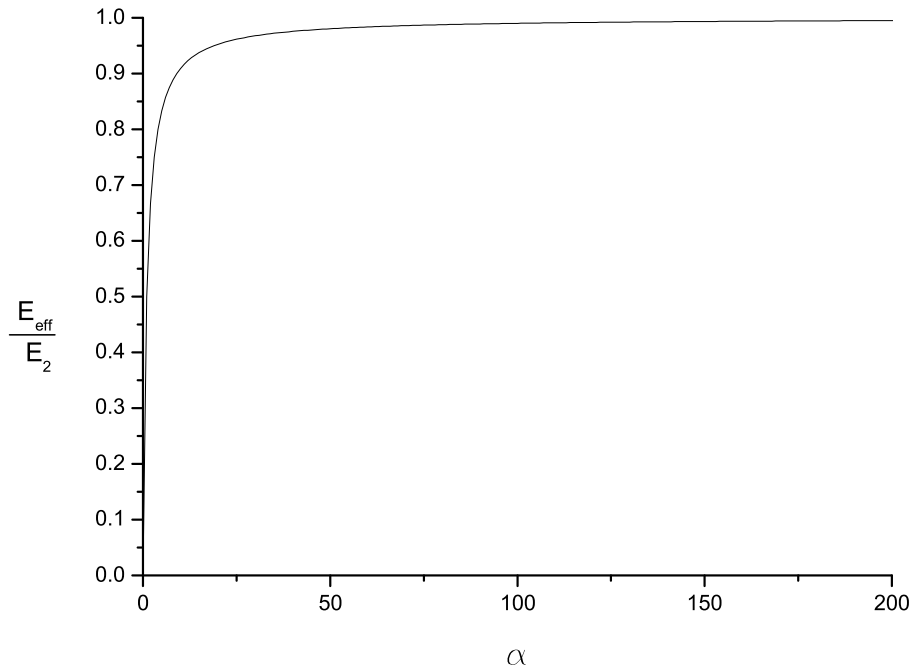


Fig. 4. Ratio between the equivalent elastic modulus and the Young's modulus of the material, as a function of the parameter  $\alpha$ .

The use of equation (13) is preferable to guidelines presented in previous work [13]-[15] because it results from mechanical considerations, and it provides a sufficient stiffness ( $\alpha$  times the stiffness of the material) while avoiding spurious oscillations caused by an excessively stiff interface. The values of the interface stiffness obtained with equation (13) and those used by other authors for a carbon/epox composite are shown in Table 3. The material's transverse modulus is  $11\text{kN/mm}^2$ , its nominal interfacial strength is  $\tau^0 = 45\text{N/mm}^2$ , and  $\alpha = 50$  is selected.

Table 3. Interface stiffness  $K$  proposed by different authors ( $\text{N/mm}^3$ ).

$t(\text{mm})$	0.125	1	2	3	5
Equation (13)	$4.43 \times 10^6$	$5.5 \times 10^5$	$2.75 \times 10^5$	$1.83 \times 10^5$	$1.1 \times 10^5$
Zou et al. [14]		$4.5 \times 10^5$	$\leq K \leq$	$4.5 \times 10^8$	
Camanho and Dávila [15]	$10^6$	$10^6$	$10^6$	$10^6$	$10^6$

Equation (13) gives a range of the interface stiffness between  $10^5$  and  $5 \times 10^6 \text{N/mm}^3$  for a sub-laminate thickness between 0.125mm and 5mm. These values are

close to the interface stiffness proposed by Camanho and Dávila and the values obtained with Zou's guidelines (between  $4.5 \times 10^5$  and  $4.5 \times 10^8 \text{N/mm}^3$ ).

(b) *Length of the cohesive zone*

Under single-mode loading, interface damage initiates at a point where the traction reaches the maximum nominal interfacial strength,  $\tau^0$ . For mixed-mode loading, interface damage onset is predicted by a criterion established in terms of the normal and shear tractions. According to Fracture Mechanics, cracks propagate when the energy release rate reaches a critical value  $G_c$ . The CZM approach prescribes the interfacial normal and shear tractions that resist separation and relative sliding at an interface. The tractions, integrated to complete separation, yield the fracture energy release rate,  $G_c$ . The length of the cohesive zone  $l_{cz}$  is defined as the distance from the crack tip to the point where the maximum cohesive traction is attained (see Figure 5).

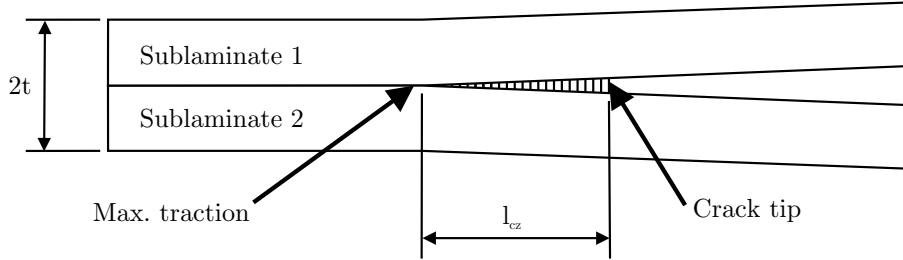


Fig. 5. *Length of the cohesive zone.*

Different models have been proposed in the literature to estimate the length of the cohesive zone. Irwin [18] estimated the size of the plastic zone ahead of a crack in a ductile solid by considering the crack tip zone within which the von Mises equivalent stress exceeds the tensile yield stress. Dugdale [4] estimated the size of the yield zone ahead of a mode I crack in a thin plate of an elastic-perfectly plastic solid by idealizing the plastic region as a narrow strip extending ahead of the crack tip that is loaded by the yield traction. Barenblatt [5] provided an analogue for ideally brittle materials of the Dugdale plastic yield zone analysis. Hui [19] estimated the length of the cohesive zone for soft elastic solids, and Falk [12] and Rice [20] estimated the length of the cohesive zone as a function of the crack growth velocity. The expressions that result from these models for the case of plane stress are presented in Table 4. It is assumed that the relation between the critical stress intensity factor  $K_c$  and the critical energy release rate  $G_c$  can be expressed as  $K_c^2 = G_c E$ .

All the models described above to predict the cohesive zone length  $l_{cz}$  have the form:

$$l_{cz} = ME \frac{G_c}{(\tau^0)^2} \quad (14)$$

where  $E$  is the Young modulus of the material,  $G_c$  is the fracture energy release rate,  $\tau^0$  is the maximum interfacial strength, and  $M$  is a parameter that depends on each model. The most commonly used models in the literature are Hillerborg's model [6] and Rice's model [20]. In these models, the parameter  $M$  is either close or exactly equal to unity. A summary of the different models commonly used in the literature, and the equivalent parameter  $M$  for plane stress are shown in Table 4. In this paper, Hillerborg's model is used.

For the case of orthotropic materials with transverse isotropy, the value of the Young's modulus in equation (14) is the transverse modulus of the material,  $E_2$ .

Table 4. Length of the cohesive zone and equivalent value of the parameter  $M$ .

	$l_{cz}$	$M$
Hui [19]	$\frac{2}{3\pi} E \frac{G_c}{(\tau^0)^2}$	0.21
Irwin [18]	$\frac{1}{\pi} E \frac{G_c}{(\tau^0)^2}$	0.31
Dugdale [4], Barenblatt [5]	$\frac{\pi}{8} E \frac{G_c}{(\tau^0)^2}$	0.4
Rice [20], Falk [12]	$\frac{9\pi}{32} E \frac{G_c}{(\tau^0)^2}$	0.88
Hillerborg [6]	$E \frac{G_c}{(\tau^0)^2}$	1

In order to obtain accurate results using CZM, the tractions in the cohesive zone must be represented adequately by the finite element spatial discretization. The number of elements in the cohesive zone is obtained with the equation:

$$N_e = \frac{l_{cz}}{l_e} \quad (15)$$

where  $l_e$  is the mesh size in the direction of crack propagation.

When the cohesive zone is discretized by too few elements, the fracture energy is not represented accurately and the model does not capture the continuum field of a cohesive crack. Therefore, a minimum number of elements,  $N_e$ , is needed in the cohesive zone to get successful FEM results.

However, the minimum number of elements needed in the cohesive zone is not well established: Moës and Belytschko [21], based on the work of Carpinteri and Cornetti [22], suggest using more than 10 elements. However, Falk

et al. [12] used between 2 and 5 elements in their simulations. In the parametric study by Dávila and Camanho [23], the minimum element length for predicting the delamination in a double cantilever beam (DCB) specimen was 1mm, which leads, using equation (14), to a length of the cohesive zone of 3.28mm. Therefore, 3 elements in the cohesive zone were sufficient to predict the propagation of delamination in Mode I.

### 2.3 Guidelines for the selection of the parameters of the interface with coarser mesh

One of the drawbacks in the use of cohesive zone models is that very fine meshes are needed to assure a reasonable number of elements in the cohesive zone. The length of the cohesive zone given by equation (14) is proportional to the fracture energy release rate ( $G_c$ ) and to the inverse of the square of the interfacial strength  $\tau^0$ . For typical graphite-epoxy or glass-epoxy composite materials, the length of the cohesive zone is smaller than one or two millimeters. Therefore, according to equation (15), the mesh size required in order to have more than two elements in the cohesive zone should be smaller than half a millimeter. The computational requirements needed to analyze a large structure with these mesh sizes may render most practical problems intractable.

Alfano and Crisfield [24] observed that variations of the maximum interfacial strength do not have a strong influence in the predicted results, but that lowering the interfacial strength can improve the convergence rate of the solution. The result of using a lower interfacial strength is that the length of the cohesive zone and the number of elements in the cohesive zone increase. Therefore, the representation of the softening response ahead of a crack tip is more accurate with a lower interface strength.

It is possible to develop a strategy to adapt the length of the cohesive zone to a given mesh size. The procedure consists of determining the value  $\bar{\tau}^0$  of the interfacial strength required for a desired number of elements ( $N_e^0$ ) in the cohesive zone. From equations (14) and (15), the required interface strength is:

$$\bar{\tau}^0 = \sqrt{\frac{EG_c}{N_e^0 l_e}} \quad (16)$$

Finally, the interfacial strength is chosen as:

$$T = \min \{ \tau^0, \bar{\tau}^0 \} \quad (17)$$

The effect of a reduction of the interfacial strength is to enlarge the cohesive

zone, and thus, the model is better suited to capture the softening behaviour ahead of the crack tip. Moreover, if equation (13) is used to compute the interface stiffness, the interface stiffness will be large enough to assure a stiff connection between the two neighboring layers and small enough to avoid spurious oscillations. The drawback associated with reducing the interfacial strength is that the stress distribution in the regions near the crack tip may not be accurate [24].

### 3 Simulation of the double cantilever beam specimen

The influence of mesh size, interface stiffness, and interface strength were investigated by analyzing the Mode I test of a double cantilever beam (DCB). The DCB specimen was fabricated with a unidirectional T300/977-2 carbon-fiber-reinforced epoxy laminate. The specimen is 150-mm-long, 20.0 mm-wide, with two 1.98-mm-thick arms, and an initial crack length of 55mm. The material properties are shown in Table 5 [25].

Table 5. Mechanical and interface material properties of T300/977-2.

$E_{11}$	$E_{22} = E_{33}$	$G_{12} = G_{13}$	$G_{23}$
150.0GPa	11.0GPa	6.0GPa	3.7GPa
$\nu_{12} = \nu_{13}$	$\nu_{23}$	$G_{IC}$	$\tau_3^0$
0.25	0.45	0.352N/mm	60MPa

The FEM model was composed of two layers of four-noded 2D plane strain elements connected together with four-node decohesion elements. The decohesion elements were implemented using a user-written subroutine in the finite element code ABAQUS [26].

Three sets of simulations were performed. First, a DCB test was simulated with different levels of mesh refinement using the material properties shown in Table 5 and interfacial stiffness of  $K=10^6\text{N/mm}^3$ . Then, equations (15) and (13) were used to calculate an adjusted interfacial strength and interface stiffness. Finally, a set of simulations with a constant mesh size using different interface stiffnesses in order to investigate the influence of the stiffness on the calculated results.

Several analyses were carried out for mesh sizes ranging between 0.125mm and 5mm. The load-displacement curves obtained for different element sizes using the nominal interfacial strength are shown in Figure 6.

The results indicate that a mesh size of  $l_e \leq 0.5\text{mm}$  is necessary to obtain converged solutions. The predictions made with coarser meshes significantly overpredict the experimental results.

The length  $l_{cz}$  of the cohesive zone for the material given in Table 5 is close to 1mm. For a mesh size greater than 0.5mm, fewer than two elements would span the cohesive zone, which is not sufficient for an accurate representation [22]-[23]. For a mesh size smaller than 0.5mm, more than two elements would span the cohesive zone. For a mesh size of 0.25mm, four elements would span the cohesive zone.

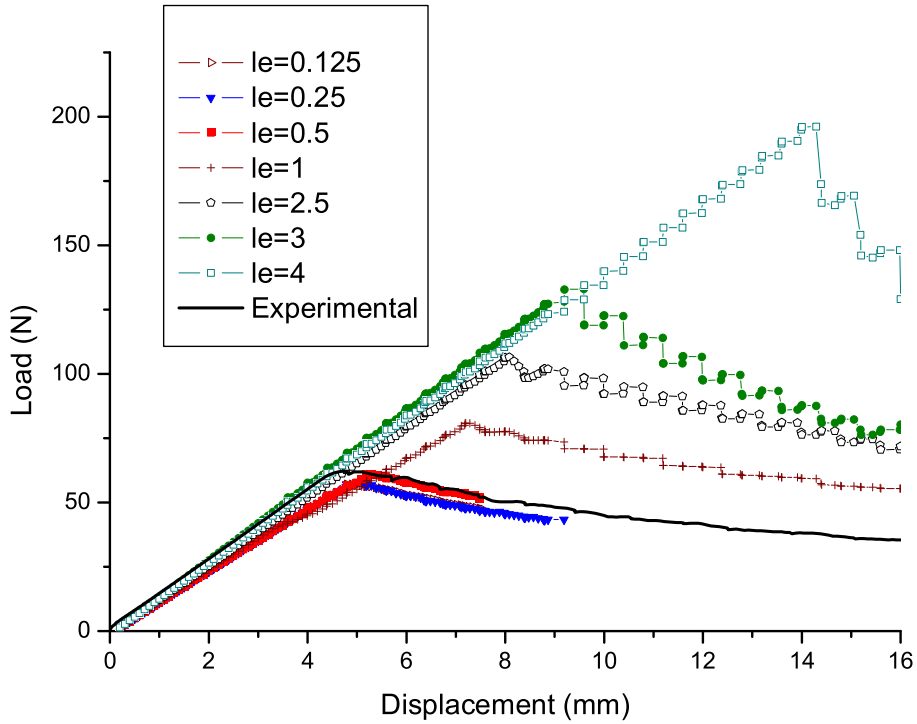


Fig. 6. Load-displacement curves obtained for a DCB test with different mesh sizes.

### 3.1 Effect of interface strength

To verify the effect of interface strength on the computed results, simulations were performed by specifying the desired number of elements within the cohesive zone to be  $N_0 = 5$  and reducing the interface strength according to equation (17). The load-displacement curves obtained for several levels of mesh refinement are shown in Figure 7. Accurate results are obtained for mesh sizes smaller than 2.5mm.

A comparison of the load-displacement curves for the DCB specimen calculated using the nominal interface strength and the strength obtained from

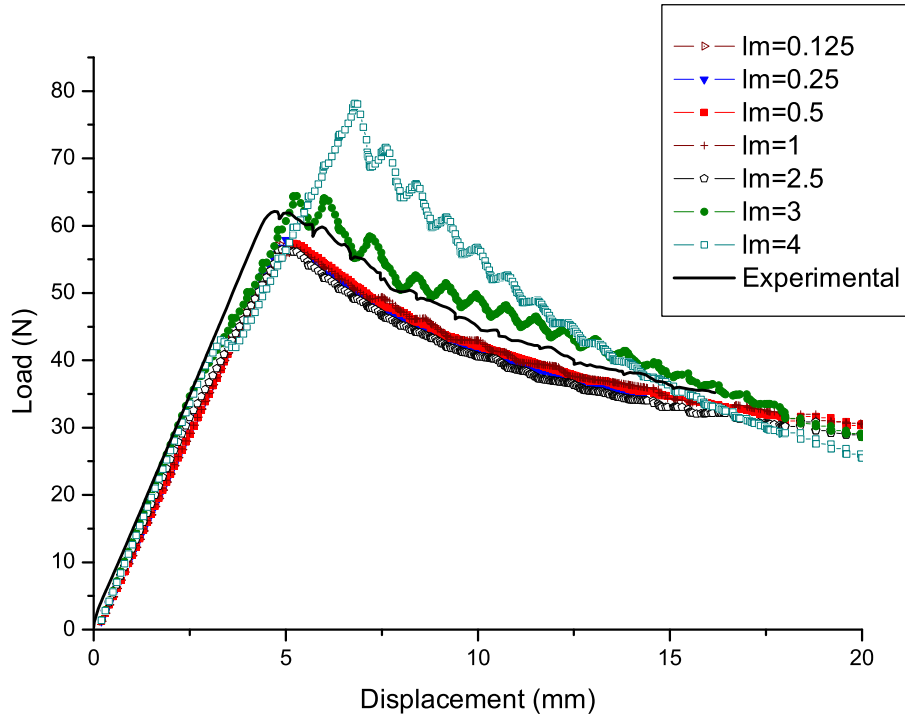


Fig. 7. Load-displacement curves obtained for a DCB test with different mesh sizes and keeping constant the number of elements (5) in the cohesive zone.

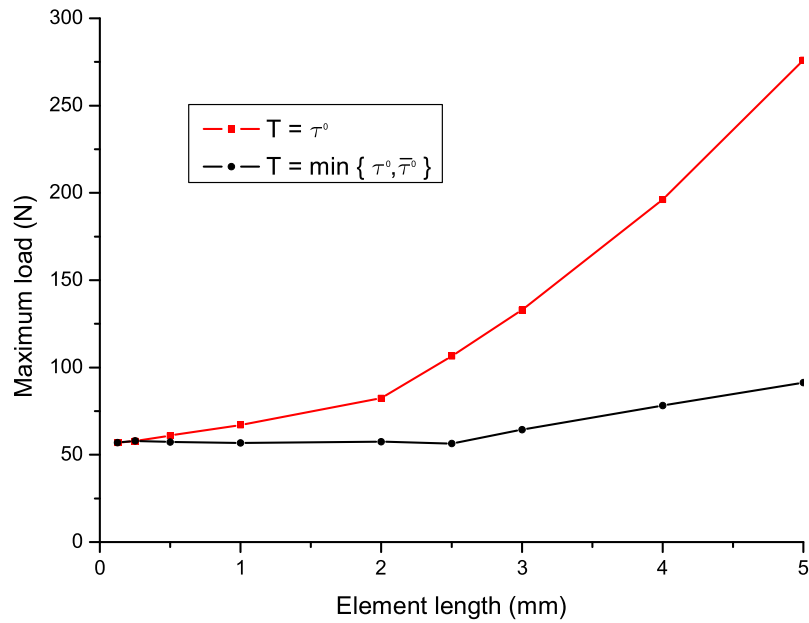


Fig. 8. Maximum load obtained in a DCB test for two cases: a) with constant interfacial strength, b) with interfacial strength calculated according to Eq. (17).

equation (17) is shown in Figure 8. The maximum load obtained by keeping the maximum interfacial strength constant increases with the mesh size, so the results obtained are mesh dependent, especially for mesh sizes greater than 2mm. However, the loads predicted by modifying the interfacial strength according to equation (17) are nearly constant for element sizes smaller than 3mm. In addition, the global deformation and the crack tip position are also nearly independent for mesh refinement, as illustrated in Figure 9.

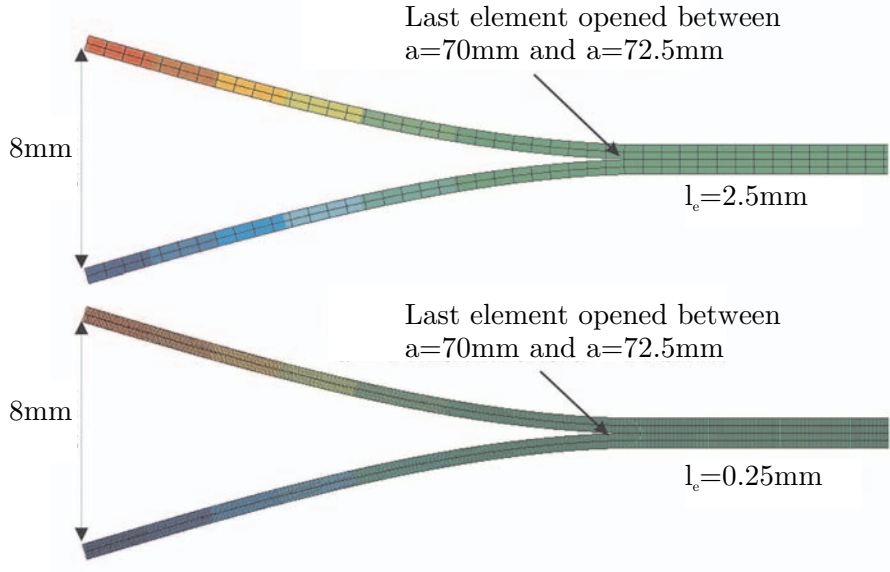


Fig. 9. Crack tip for different element size.

### 3.2 Effect of interface stiffness

The DCB test was simulated with a mesh size of 2.5mm for various values of the interface stiffness in order to investigate the influence of the stiffness on the predicted failure load. The results of the simulations are presented in Figure 10.

The load-displacement response curves obtained from simulations using an interface stiffness greater than  $10^4\text{N/mm}^3$  are virtually identical. However, smaller values of the interface stiffness have a strong influence on the load-displacement curves, since a stiff connection between the two neighboring layers is not assured. Moreover, the number of iterations needed for the solution when using an interface stiffness smaller than  $10^4\text{N/mm}^3$  is greater than the number of iterations needed for range of the interface stiffness between  $10^6$  and  $10^{10}\text{N/mm}^3$ . For values of the interface stiffness significantly greater than  $10^{10}\text{N/mm}^3$ , the number of iterations needed for the solution increases (see

Figure 11). The stiffness that results from equation (13) is  $5.55 \times 10^5 \text{ N/mm}^3$ , which is ideal for good convergence of the solution procedure.

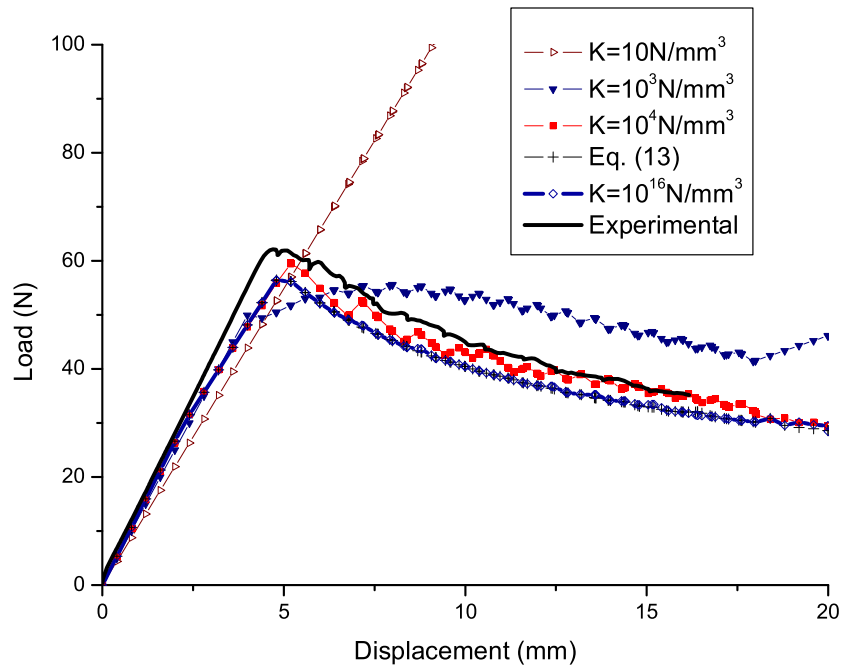


Fig. 10. Influence of the value of the interface stiffness on the load-displacement curves.

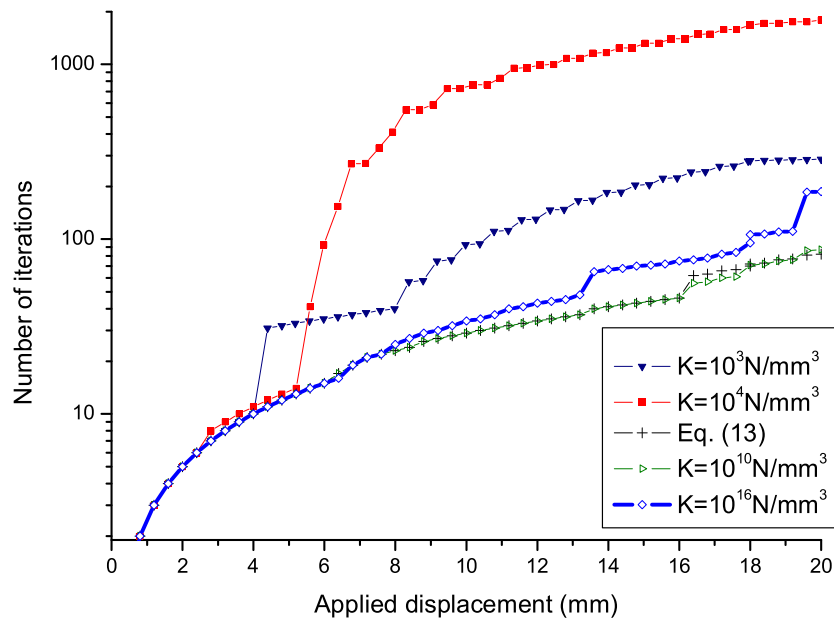


Fig. 11. Influence of the value of the interface stiffness on the number of iterations.

## 4 Concluding remarks

An engineering solution for the simulation of delamination using coarse meshes was presented. Two new guidelines for the selection of the parameters for the constitutive equation used for the simulation of delamination were presented.

First, a new equation for the selection of the interface stiffness parameter  $K$  was derived. The new equation is preferable to previous guidelines because it results from mechanical considerations rather than from experience. The approach provides an adequate stiffness to ensure a sufficiently stiff connection between two neighboring layers, while avoiding the possibility of spurious oscillations in the solution caused by overly stiff connections.

Finally, an expression to adjust the maximum interfacial strength used in the computations with coarse meshes was presented. It was shown that a minimum number of elements within the cohesive zone is necessary for accurate simulations. By reducing the maximum interfacial strength, the cohesive zone length is enlarged and more elements span the cohesive zone. The results obtained by reducing the maximum interfacial strength show that accurate results can be obtained with a mesh ten times coarser than by using the nominal interface strength. The drawback in using a reduced interfacial strength value is that the stress concentrations in the bulk material near the crack tip are less accurate.

## References

- [1] Krueger, R., The virtual crack closure technique: history, approach and applications. *NASA/Contractor Report-2002-211628*, 2002.
- [2] Turon, A., Camanho, P.P., Costa, J., Dávila, C.G., An interface damage model for the simulation of delamination under variable-mode ratio in composite materials. *NASA/Technical Memorandum 213277*, 2004.
- [3] Turon, A., Camanho, P.P., Costa, J., Dávila, C.G., A damage model for the simulation of delamination in advanced composites under variable-mode loading. *Mechanics of Materials*, submitted, 2005.
- [4] Dugdale, D.S., Yielding of steel sheets containing slits. *Journal of the Mechanics and Physics of Solids* **8**, 100-104. 1960.
- [5] Barenblatt, G., The mathematical theory of equilibrium cracks in brittle fracture. *Advances in Applied Mechanics*, **7**, 55-129. 1962.
- [6] Hillerborg, A., Modéer, M., Petersson, P.E., Analysis of crack formation and crack growth in concrete by means of fracture mechanics and finite elements. *Cement and Concrete Research*. **6**, 773-782. 1976.

- [7] Ortiz, M., Pandolfi, A., Finite-deformation irreversible cohesive elements for three- dimensional crack propagation analysis. *International Journal for Numerical Methods in Engineering*, **44**, 1267-82, 1999.
- [8] Tvergaard, V., Hutchinson, J.W., The relation between crack growth resistance and fracture process parameters in elastic-plastic solids. *Journal of Mechanics and Physics of Solids*, **40**, 1377-1397, 1992.
- [9] Cui, W., Wisnom, M. R., A combined stress-based and fracture-mechanics-based model for predicting delamination in composites. *Composites*, **24**, 467-474, 1993.
- [10] Needleman, A., A continuum model for void nucleation by inclusion debonding. *Journal of Applied Mechanics*, **54**, 525-532, 1987.
- [11] Xu X-P, Needleman, A., Numerical simulations of fast crack growth in brittle solids. *Journal of Mechanics and Physics of Solids*, **42** (9), 1397-1434, 1994.
- [12] Falk, M.L., Needleman, A., Rice J.R., A critical evaluation of cohesive zone models of dynamic fracture. *Journal de Physique IV, Proceedings*, 543-550, 2001.
- [13] Daudeville, L., Allix, O., Ladevèze, P., Delamination analysis by damage mechanics. Some applications. *Composites Engineering*, **5**(1), 17-24, 1995.
- [14] Zou, Z., Reid, S.R., Li, S., Soden, P.D., Modelling interlaminar and intralaminar damage in filament wound pipes under quasi-static indentation. *Journal of Composite Materials*, **36**, 477-499, 2002.
- [15] Camanho, P.P., Dávila, C.G., de Moura M.F. Numerical simulation of mixed-mode progressive delamination in composite materials. *Journal of Composite Materials*, **37** (16), 1415-1438, 2003.
- [16] Klein, P.A., Foulk, J.W., Chen, E.P., Wimmer, S.A., Gao, H., Physics-based modeling of brittle fracture: cohesive formulations and the application of meshfree methods. *Sandia Report SAND2001-8099*, 2000.
- [17] Schellekens, J.C.J., de Borst, R., A nonlinear finite-element approach for the analysis of mode-I free edge delamination in composites. *International Journal for Solids and Structures*, **30**(9), 1239-1253, 1993.
- [18] Irwin, G.R., Plastic zone near a crack and fracture toughness. In *Proceedings of the Seventh Sagamore Ordnance Materials Conference*, vol. **IV**, 63-78, New York: Syracuse University, 1960.
- [19] Hui, C.Y., Jagota, A., Bennison, S.J., Londono, J.D., Crack blunting and the strength of soft elastic solids. *Proceedings of the Royal Society of London A*, **459**, 1489-1516, 2003.
- [20] Rice, J.R., The mechanics of earthquake rupture. *Physics of the Earth's Interior (Proc. International School of Physics "Enrico Fermi"*, Course 78, 1979; ed. A.M. Dziewonski and E. Boschi), Italian Physical Society and North-Holland Publ. Co., 555-649, 1980.

- [21] Moës, N., Belytschko, T., Extended finite element method for cohesive crack growth. *Engineering Fracture Mechanics*, **69**,813-833, 2002.
- [22] Carpinteri, A., Cornetti, P., Barpi, F., Valente, S., Cohesive crack model description of ductile to brittle size-scale transition: dimensional analysis vs. renormalization group theory. *Engineering Fracture Mechanics*, **70**, 1809-1939, 2003.
- [23] Dávila, C.G., Camanho, P.P., de Moura, M.F.S.F., Mixed-Mode decohesion elements for analyses of progressive delamination. *Proceedings of the 42nd AIAA/ASME/ASCE/AHS/ASC Structures, Structural Dynamics and Materials Conference*, Seattle, Wasington, April 16-19, 2001.
- [24] Alfano, G., Crisfield, M.A., Finite element interface models for the delamination analysis of laminated composites: mechanical and computational issues. *International Journal for Numerical Methods in Engineering*, **77**(2), 111-170, 2001.
- [25] Morais, A.B., de Moura, M.F., Marques, A.T., de Castro, P.T., Mode-I interlaminar fracture of carbon/epoxy cross-ply composites. *Composites Science and Technology*, **62**, 679-686, 2002.
- [26] Hibbitt, Karlsson, Sorensen. ABAQUS 6.2 User's Manuals. Pawtucket, USA, 1996.

REPORT DOCUMENTATION PAGE				Form Approved OMB No. 0704-0188	
<p>The public reporting burden for this collection of information is estimated to average 1 hour per response, including the time for reviewing instructions, searching existing data sources, gathering and maintaining the data needed, and completing and reviewing the collection of information. Send comments regarding this burden estimate or any other aspect of this collection of information, including suggestions for reducing this burden, to Department of Defense, Washington Headquarters Services, Directorate for Information Operations and Reports (0704-0188), 1215 Jefferson Davis Highway, Suite 1204, Arlington, VA 22202-4302. Respondents should be aware that notwithstanding any other provision of law, no person shall be subject to any penalty for failing to comply with a collection of information if it does not display a currently valid OMB control number.</p> <p><b>PLEASE DO NOT RETURN YOUR FORM TO THE ABOVE ADDRESS.</b></p>					
1. REPORT DATE (DD-MM-YYYY)		2. REPORT TYPE		3. DATES COVERED (From - To)	
01- 03 - 2005		Technical Memorandum			
4. TITLE AND SUBTITLE An Engineering Solution for Using Coarse Meshes in the Simulation of Delamination With Cohesive Zone Models				5a. CONTRACT NUMBER	
				5b. GRANT NUMBER	
				5c. PROGRAM ELEMENT NUMBER	
6. AUTHOR(S) Turon, Albert; Dávila, Carlos G.; Camanho, Pedro P.; and Costa, Josep				5d. PROJECT NUMBER	
				5e. TASK NUMBER	
				5f. WORK UNIT NUMBER 23-064-30-22	
7. PERFORMING ORGANIZATION NAME(S) AND ADDRESS(ES) NASA Langley Research Center Hampton, VA 23681-2199				8. PERFORMING ORGANIZATION REPORT NUMBER  L-19109	
9. SPONSORING/MONITORING AGENCY NAME(S) AND ADDRESS(ES) National Aeronautics and Space Administration Washington, DC 20546-0001				10. SPONSOR/MONITOR'S ACRONYM(S)  NASA	
				11. SPONSOR/MONITOR'S REPORT NUMBER(S)  NASA/TM-2005-213547	
12. DISTRIBUTION/AVAILABILITY STATEMENT Unclassified - Unlimited Subject Category 39 Availability: NASA CASI (301) 621-0390					
13. SUPPLEMENTARY NOTES Turon and Costa: University of Girona; Dávila: Langley Research Center; Camanho: University of Porto. An electronic version can be found at <a href="http://ntrs.nasa.gov">http://ntrs.nasa.gov</a>					
14. ABSTRACT  This paper presents a methodology to determine the parameters used in the simulation of delamination in composite materials using decohesion finite elements. A closed-form expression is developed to define the stiffness of the cohesive layer. A novel procedure that allows the use of coarser meshes of decohesion elements in large-scale computations is proposed. The procedure ensures that the energy dissipated by the fracture process is correctly computed. It is shown that coarse-meshed models defined using the approach proposed here yield the same results as the models with finer meshes normally used in the simulation of fracture processes.					
15. SUBJECT TERMS Progressive delamination; Decohesion elements; Laminated composites; Debonding; Continuum Damage Mechanics					
16. SECURITY CLASSIFICATION OF:			17. LIMITATION OF ABSTRACT	18. NUMBER OF PAGES	19a. NAME OF RESPONSIBLE PERSON
a. REPORT	b. ABSTRACT	c. THIS PAGE			STI Help Desk (email: <a href="mailto:help@sti.nasa.gov">help@sti.nasa.gov</a> )
U	U	U	UU	26	19b. TELEPHONE NUMBER (Include area code) (301) 621-0390